J Intell Manuf (2014) 25:157–163
DOI 10.1007/s10845-012-0682-1

Bead geometry prediction for robotic GMAW-based rapid manufacturing through a neural network and a second-order regression analysis

Jun Xiong · Guangjun Zhang · Jianwen Hu · Lin Wu

Received: 28 December 2011 / Accepted: 4 July 2012 / Published online: 19 July 2012

Abstract The single weld bead geometry has critical effects on the layer thickness, surface quality, and dimensional accuracy of metallic parts in layered deposition process. The present study highlights application of a neural network and a second-order regression analysis for predicting bead geometry in robotic gas metal arc welding for rapid manufacturing. A series of experiments were carried out by applying a central composite rotatable design. The results demonstrate that not only the proposed models can predict the bead width and height with reasonable accuracy, but also the neural network model has a better performance than the second-order regression model due to its great capacity of approximating any nonlinear processes. The neural network model can efficiently be used to predict the desired bead geometry with high precision for the adaptive slicing principle in layer additive manufacturing.

Keywords Rapid prototyping · Gas metal arc welding · Weld bead geometry · Neural network · Regression analysis

Introduction

Layered deposition manufacturing, also known as rapid prototyping (RP), has gained worldwide popularity due to its capability of forming 3D metal components directly from original prototype of products. Many ongoing researches focus on making metallic parts with laser welding and gas metal arc welding (GMAW). The advantages of using focused laser beam as the heat source are low thermal input, less distortion of parts. But its effective utilization of energy is very poor (Unocic and DuPont 2004). It also requires a complex production device and an expensive wire feeding system. Recently, the RP system based on GMAW interested many researchers as it can fabricate fully dense components with high efficiency and low cost. Furthermore, metallic parts deposited with GMAW process have the advantages of excellent mechanical performance, high density and favorable bonding strength (Mughal et al. 2006).

The essence of RP based on robotic GMAW process is that a welding arc is employed as the energy source to melt metal wire on a substrate, which is also known as the full weld deposition technology. Doumanidis and Kwak (2002) developed a multivariable adaptive modeling and control process of bead size in GMAW material deposition with application in solid freeform fabrication (SFF), and a cylindrical metal part was formed. Zhang et al. (2003) employed GMAW as a deposition technology to establish a RP system including planning/slicing, system implement and metal transfer control. Song and Park (2006) integrated the application of 3D welding and milling to improve the surface quality and dimensional accuracy of SFF parts. Karunakaran et al. (2010) developed a hybrid layered manufacturing technology that combines GMAW for layered deposition and CNC machining as a subtractive technique to build metallic objects.

Usually, the key idea of RP is an additive layered manufacturing process that slices complicated 3D geometry into simple 2.5D features, without part-specific fixture or tooling (Weiss et al. 1992). An intelligent RP system, including development of 3D models of objects, planning and slicing of expected thickness for each layer, design of the welding path and process parameters in each layer, communication with the robot, accumulation of weld beads by layers, real time detection and control of bead geometry, is shown in Fig. 1. In order to realize the adaptive slicing principle of RP, the

J. Xiong · G. Zhang (✉) · J. Hu · L. Wu
State Key Laboratory of Advanced Welding and Joining, Harbin Institute of Technology, West Straight Street 92, Harbin 150001, People's Republic of China
e-mail: zhanggj@hit.edu.cn

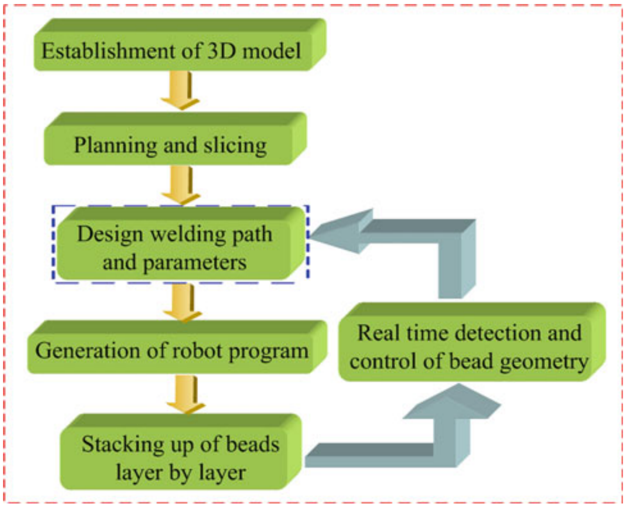

Fig. 1 The schema of intelligent RP system

relationship between process variables and bead geometry should be studied for setting the optimum welding parameters of designed weld beads. This is because the single weld bead geometry plays a major role in the determination of surface smoothness, layer thickness, and dimensional accuracy of deposited parts. The dependence of the weld bead geometry on welding parameters is significant. The process parameters are selected purely based on human experience or a data book. However, this may not produce an expected bead size. It is essential to develop models relating process variables to the bead geometry.

In recent years, many methods can be used to relate the relationship between process variables and responses, such as factorial design, linear regression, second-order regression, Taguchi method, and artificial network. However, the accuracy of linear regression method for predicting responses is not adequate. Taguchi method can not lead to an optimal solution. Factorial design method needs a large number of experiments. Artificial neural network (ANN) and second-order regression methods have been demonstrated to be powerful tools to establish models of welding process. The ANN exhibits a great capacity to perform nonlinear and multivariable mappings. Moreover, a neural network can accurately represent complicated relationships between multiple inputs and outputs. Nagesh and Datta (2002) investigated the process variables selection for the optimization of bead geometry through neural networks in shielded metal-arc welding. Huang and Kovacevic (2011) optimized the weld penetration in laser welding based on acoustic signatures by means of the ANN optimization model. A well trained neural network was used to optimize the weld bead geometry in a novel GMAW process (Lin 2010). Chokkalingham et al. (2011) predicted the bead depth from the infra red thermal image of the weld pool by means of a neural network model. While the conventional regression analysis establishes models using a standard statistical technique. Murugan and Gunaraj (2005) developed the relationship between weld bead width, height and penetration with process parameters for submerged arc welding pipes. Kannan and Yoganandh (2010) established mathematical models to predict the clad bead geometry in GMAW by means of response surface methodology.

However, these models usually regard depth of penetration for good fusion as the major consideration in joining applications. Little has been done to discuss the modeling of GMAW-based deposition process systematically. The Taguchi approach has been used to investigate the effect of process parameters on the bead quality in RP process (Sreenathbabu et al. 2005; Song et al. 2005). This optimization method works through calculating signal-to-noise (SN) ratios for each combination of process variables. It can only generate optimal solutions within the prescribed parameter levels. The optimal level does not always find an optimum solution. In this study, the prediction of the bead geometry in layered deposition process is carried out by means of a neural network and a second-order regression analysis. Based on the developed models, the bead geometry can be predicted and optimized with various control variables. Consequently, an adaptive slicing principle of RP can be achieved in the near future.

Experimental details

Experimental setup

A schematic diagram of the experimental details is shown in Fig. 2. During the experiments, a Fronius make welding machine (TPS5000) was used as the power source. And a motoman UP20 robot manipulator was applied to control the welding path. The GMAW deposition produced molten weld droplets by heating with an arc between a consumable electrode and the substrate. The electrode of 1.2 mm was a copper coated steel wire with composition C (0.11 % maximum), Mn (1.8–2.1 %), Si (0.65–0.95), Cr (0.2 maximum) and Ni (0.3 maximum). The shielding gas was Ar (95 %) and CO_2 (5 %) mixture at a constant flow rate of 18 l/min. A mild steel with dimension of 210 mm × 120 mm × 9.5 mm was employed as the substrate to deposite single weld beads.

Identification of input process parameters and response variables

Four independently input process parameters were wire feed rate (F), welding speed (S), arc voltage (V), and nozzle-to-plate distance (D). The chosen responses were bead width (W) and bead height (H), as depicted in Fig. 3. The working limits of the input parameters were fixed by carrying on trial

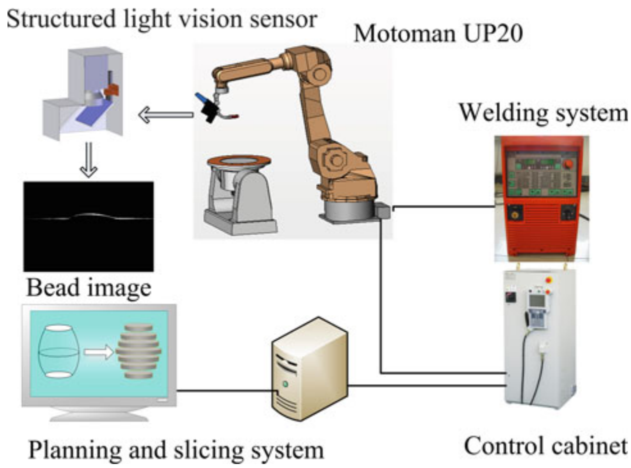

Fig. 2 Schematic diagram of the experimental set-up

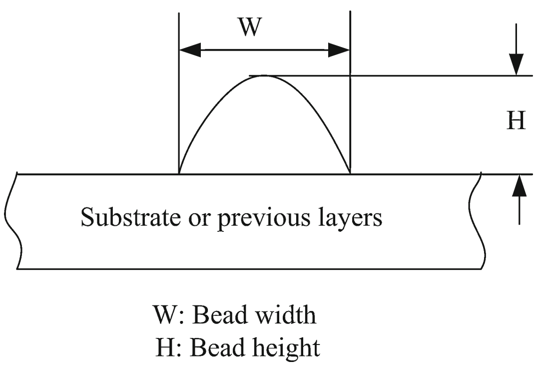

Fig. 3 Weld bead geometry

runs, through inspecting weld beads for smooth appearance and no obvious imperfection. It is known that heat accumulation is serious in the RP process. So less thermal input and better heat distribution play a major role in weld-based deposition because excessive heat may remelt the former layer and alter the previous bead shapes. Thus, a lower wire feed rate and a higher torch speed are expected. The values and units of the chosen process variables at various levels are presented in Table 1. It should be noted that the arc voltage is designed from 16 to 22 V. 16 V is just a low limit and is seldom used in practical applications.

Development of the experimental design matrix

The design matrix to conduct the experiments was a central composite rotatable design, which is able to decrease costs and to provide the necessary information concerning the main and interaction effects on the response factors (Montgomery 2003). The experimental design matrix is shown in Table 2. It includes sixteen experiments as factorial points, eight experiments as star points and seven experiments as center points.

Table 1 Process parameters and their limits

Parameters	Symbol	Factor levels				
		Level 1	Level 2	Level 3	Level 4	Level 5
Wire feed rate (m/min)	F	2.8	3.6	4.4	5.2	6.0
Welding speed (cm/min)	S	15.0	22.5	30.0	37.5	45.0
Arc voltage (V)	V	16.0	17.5	19.0	20.5	22.0
Nozzle-to-plate distance (mm)	D	6.0	9.0	12.0	15.0	18.0

Recording the response variables

A laser structured light vision sensor, projecting a laser line on the weld bead cross-section, was used to determine the bead width and height of the single bead, as seen in Fig. 2. The vision sensor was composed of a laser projector with power of 30 mW emitting at 650 nm, and a CCD camera. With a view to reducing noises, a narrow-band filter with same center wavelength of the laser diode and a neutral filter were placed in front of the camera. The camera is capable of collecting 8 bit gray scale images. A center of gravity method was applied to process images for acquiring the center line of the laser stripe. The feature points of the laser line were extracted by the maximum distance method. The sensor was calibrated precisely by means of an accurately machined steel bar with step gradations. Every bead geometry was measured for three times at different locations away from arc striking and extinguishing points to eliminate the end effects. The average of the three measurements was used as the corresponding response.

Neural network modeling

Artificial networks have been demonstrated to be efficient tools to deal with complicated and highly interactive processes by using experimental data without any assumptions. In this work, a neural network was adopted to characterize the complex relationship between input variables and the bead geometry.

The structure of the neural network was a multilayer feedforward network which is normally trained with the back-propagation error algorithm. The multilayer feedforward network has the capability of approximating any nonlinear processes. A schematic representation of the structure of the multilayer feedforward network that performs the mapping between the four input process variables and two output responses is shown in Fig. 4. The network was composed of an input layer, a hidden layer and an output layer.

Table 2 Design matrix and responses

S. no	Design matrix				W (mm)	H (mm)
	F (m/min)	S (cm/min)	V (V)	D (mm)		
1	3.6	22.50	17.50	9.00	8.95	2.88
2	5.20	22.50	17.50	9.00	10.72	3.35
3	3.60	37.50	17.50	9.00	7.19	2.45
4	5.20	37.50	17.50	9.00	8.29	2.75
5	3.60	22.50	20.50	9.00	10.25	2.66
6	5.20	22.50	20.50	9.00	11.5	3.26
7	3.60	37.50	20.50	9.00	8.36	2.17
8	5.20	37.50	20.50	9.00	9.35	2.58
9	3.60	22.50	17.50	15.00	8.36	3
10	5.20	22.50	17.50	15.00	9.52	3.56
11	3.60	37.50	17.50	15.00	6.83	2.45
12	5.20	37.50	17.50	15.00	7.98	2.9
13	3.60	22.50	20.50	15.00	9.92	2.79
14	5.20	22.50	20.50	15.00	11.12	3.35
15	3.60	37.50	20.50	15.00	7.91	2.26
16	5.20	37.50	20.50	15.00	9.25	2.7
17	2.80	30.00	19.00	12.00	7.39	2.32
18	6.00	30.00	19.00	12.00	9.9	3.28
19	4.40	15.00	19.00	12.00	11.76	3.8
20	4.40	45.00	19.00	12.00	7.54	2.34
21	4.40	30.00	16.00	12.00	8.08	2.94
22	4.40	30.00	22.00	12.00	9.9	2.45
23	4.40	30.00	19.00	6.00	9.51	2.77
24	4.40	30.00	19.00	18.00	8.58	2.83
25	4.40	30.00	19.00	12.00	8.88	2.75
26	4.40	30.00	19.00	12.00	9.09	2.83
27	4.40	30.00	19.00	12.00	8.92	2.79
28	4.40	30.00	19.00	12.00	8.91	2.75
29	4.40	30.00	19.00	12.00	8.92	2.83
30	4.40	30.00	19.00	12.00	9.02	2.81
31	4.40	30.00	19.00	12.00	8.8	2.8

Neurons in the hidden layers are computational elements accomplishing nonlinear mapping between process variables and bead geometry.

The training data of the neural work were the first 25 input-output pairs shown in Table 2. Before training the network, the data should be normalized to ensure that each welding parameter has the identical effect on the network. The linear normalization was employed as it can transform a data range to another without distortion. After linear normalization, all training data was normalized into the closed interval $[-1, 1]$.

The performance of a neural network has an important bearing on the number of hidden layers and the number of neurons in every layer. In general, a network with one hidden layer is capable of approximating any nonlinear mappings.

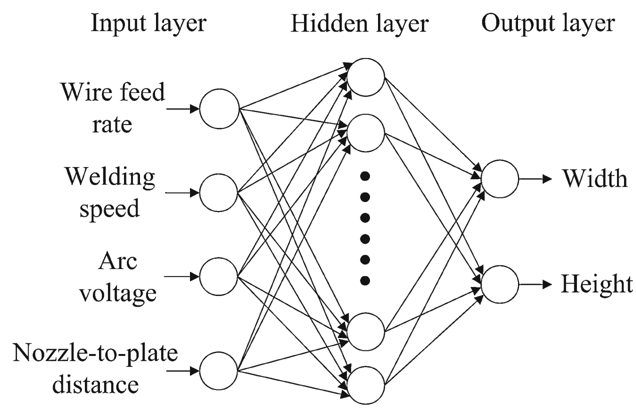

Fig. 4 A schematic diagram of a multilayer neural network

Thus, determining the number of neurons in the hidden layer is significant. Excessive hidden neurons result in overfitting and increase computational costs. On the contrary, too few hidden neurons can degrade the learning ability of the network and its approximation performance (Demuth and Beale 1998).

In this study, the development and the training of the network was performed on a PC using MATLAB application tool. The transfer function for the hidden neurons was a tangent sigmoid function and a linear function was used for the output neurons. Learning rate was set as 0.01. The number of neurons in the hidden layer was varied from 9 to 15. Different structures of the neural networks were trained. The performance function was the mean square error (MSE) minimization by updating the weights through the gradient descent approach. The best architecture was found as 4-12-2 with minimum MSE.

Second-order regression modeling

Generally, conventional regression models can be divided into linear and nonlinear regression. A second degree regression model was applied to establish the relationship between process variables and bead geometry. The response function representing any of the controllable process parameters can be expressed as (Davies 1978):

$$Y = f(X_1, X_2, X_3, X_4) \tag{1}$$

where Y is the response, e.g. bead width, height, etc. X_1 the wire feed rate (F), X_2 the welding speed (S), X_3 the arc voltage (V) and X_4 the nozzle-to-plate distance (N).

A second-order (quadratic) polynomial for the four factors is formulated as:

$$Y = \beta_0 + \sum_{i=1}^{4} \beta_i X_i + \sum_{i=1}^{4} \beta_{ii} X_i^2 + \sum_{\substack{i=1 \\ i<j}}^{4} \beta_{ij} X_i X_j \tag{2}$$

The above second-order can also be represented as follows:

$$Y = \beta_0 + \beta_1 F + \beta_2 S + \beta_3 V + \beta_4 D + \beta_{11} F^2 + \beta_{22} S^2 + \beta_{33} V^2 + \beta_{44} D^2 + \beta_{12} FS + \beta_{13} FV + \beta_{14} FD + \beta_{23} SV + \beta_{24} SD + \beta_{34} VD \quad (3)$$

where, β_0 is the constant value; $\beta_1, \beta_2, \beta_3, \beta_4$ are linear coefficients; $\beta_{11}, \beta_{22}, \beta_{33}, \beta_{44}$ are quadratic coefficients; $\beta_{12}, \beta_{13}, \beta_{14}, \beta_{23}, \beta_{24}, \beta_{34}$ are interaction coefficients.

On the basis of a statistical software (Design-expert), the values of the regression coefficients were calculated using experiment data shown in Table 2, the stepwise regression approach resulted in the following predictive equation by removing insignificant coefficients:

$$W = 8.9462 + 1.8088F - 0.3621S + 0.1739V - 0.5008D + 0.003556SD + 0.01667VD - 0.1169F^2 + 0.003137S^2 \quad (4)$$

$$H = -0.3514 + 0.4818F - 0.08477S + 0.4028V + 0.01431D - 0.006146FS + 0.001168S^2 - 0.012463V^2 \quad (5)$$

The adequacy of the developed models as well as the importance of the coefficients was validated by the analysis of variance and F-ratio. The probability values (p value) of the width and height models are less than 0.0001. The lack of fit of both models are 0.0635, 0.0702, respectively. Therefore, the developed regression equations are significant and test of goodness of fit are insignificant, namely both second-order models are adequate.

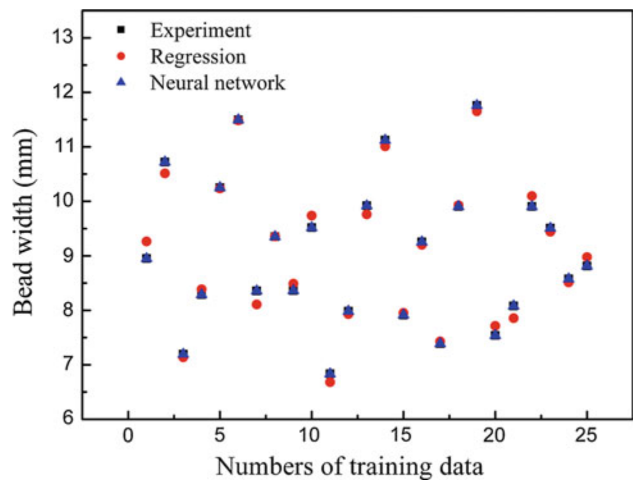

Fig. 5 Scatter diagram of predicted versus actual bead width

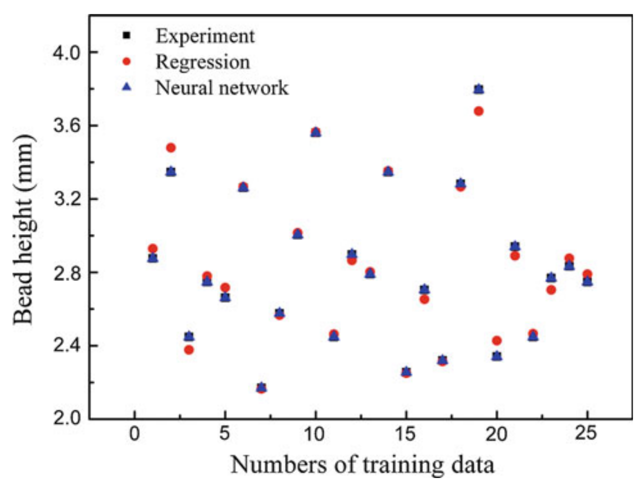

Fig. 6 Scatter diagram of predicted versus actual bead height

Selecting the most accurate model

For verifying predictable accuracy of the neutral network and the second-order regression models, the scatter diagrams of predicted versus measured bead geometry from both models by using training data are shown in Figs. 5 and 6. The performances of both models are evaluated by the mean value of the error rate (ER) and the standard deviation of the ER. The ER is defined as follows:

$$ER_{(n)} = \frac{\left|G_{predicted(n)} - G_{actual(n)}\right|}{G_{actual(n)}} \times 100\,\% \quad (6)$$

where $G_{predicted(n)}$ is the predicted bead geometry based on the model, $G_{actual(n)}$ is the measured bead geometry, and n is the experiment index.

Based on the results shown in Fig. 5, it can be observed that the widths of the weld bead achieved by different welding parameters can be predicted well by both models. The optimal network model gives the mean value and standard deviation of the ER as 0.003, 0.002 %, respectively, and the corresponding values from the regression model are 1.326, 0.976 %, respectively. Thus, the network model has a lower mean value of the ER and a lower standard deviation of ER than the results predicted from the regression model.

The result of the comparison study on the bead height between both models is displayed in Fig. 6. It is shown that the calculated values obtained using the neural network approximation show better accuracy than the regression model in most cases. The mean value and standard deviation of the ER based on the network model are 0.004, 0.003 %, respectively; the corresponding values from the regression model are 1.318, 1.163 %.

To check the accuracy of the established models in actual conditions, additional test experiments were carried out. Twelve runs were conducted using different values of process variables within their limits other than the combinations that were performed in Table 2. The process parameters and the responses from the testing experiments are shown in Table 3.

Figures 7 and 8 show the scatter diagram of predicted versus actual bead geometry from the neural network and

Table 3 Process parameters and results for the testing experiment

S. no	Process parameters				W (mm)	H (mm)
	F (m/min)	S (cm/min)	V (V)	D (mm)		
1	4	21	17	12	8.798	3.346
2	4	27	17	12	7.899	2.961
3	4	30	17	12	7.954	2.854
4	4	36	17	12	7.249	2.662
5	4	39	17	12	7.193	2.533
6	5.2	27	18.9	12	10.002	3.218
7	5.2	30	18.9	12	9.116	3.047
8	6	27	20.3	12	11.233	3.304
9	5.2	22.5	19	12	10.610	3.411
10	5.2	37.5	19	12	8.494	2.790
11	4.4	37.5	17.5	12	7.788	2.811
12	6	37.5	20.5	12	9.849	2.876

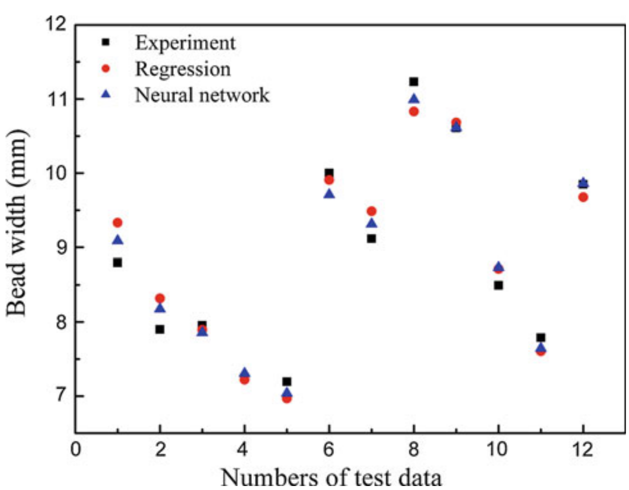

Fig. 7 Comparison of measured and calculated width

regression models by using testing data. It can be clearly seen that both models produce good fit to the experimental results and give accurate prediction of the bead width and height. A detailed error analysis for bead width and height using both models is shown in Table 4. The maximum errors of bead width and height predicted by both models are no more than 6.77 %, within the range of reasonable accuracy. For the bead width and height, the network model has a lower

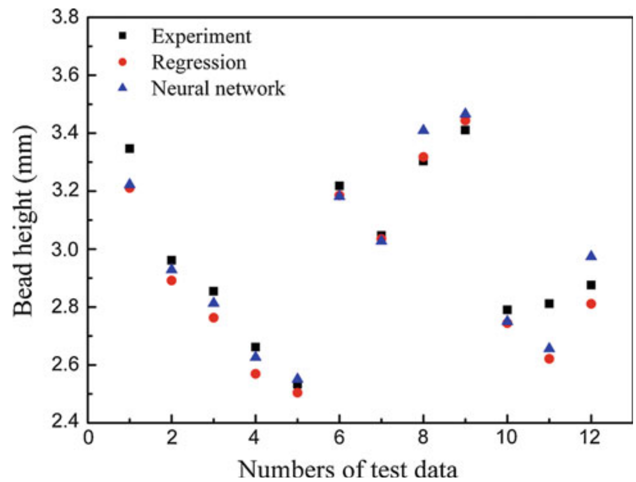

Fig. 8 Comparison of measured and calculated height

mean value and a lower standard deviation of ER than the values predicted from the second-order regression model. It can be concluded that the neural network model exhibits a better predictive ability than the regression model in actual applications. The reason why the neural network model has a better performance than the second-order regression model is that the neural network, with a hidden layer establishing a nonlinear mapping between the inputs and outputs, has strong capability of approximating any nonlinear processes.

Conclusions

This paper aims at the weld bead geometry prediction in robotic GMAW-based layer additive manufacturing. The relationships between process variables and bead geometry were investigated by a neural network and a second-order regression analysis. A series of experiments were carried out by applying a quadratic general rotary unitized design. After training different structures of neural networks, it was found that the use of a one-hidden-layer of 4-12-2 configuration model was more accurate. Then a second-order regression model was established to predict the bead geometry from the process variables. The significance and adequacy of the regression model were verified. The results indicate that the bead width and height can be predicted well by both

Table 4 Error analysis of testing data using neural network and regression model

Model	Bead width (W)			Bead height (H)		
	Maximum ER (%)	Mean of ER (%)	Standard of ER (%)	Maximum ER (%)	Mean of ER (%)	Standard of ER (%)
Neural network	3.503	1.922	1.166	5.528	2.104	1.509
Regression	6.063	2.633	1.864	6.770	2.308	1.846

models. Moreover, the neural network model has a better performance than the second-order regression model because of its strong capability of approximating any nonlinear processes. The neural network model can be applied to predict the expected bead geometry with great accuracy in layered deposition with accordance to the slicing process of RP.

Note that during the layer additive manufacturing process, a slightly increased bead width and a decreased bead height will produce due to the effect of heat accumulation. In future studies, a real time detection and closed-loop control system will be developed to make the bead geometry consistent with the designed bead geometry.

Acknowledgments This work was supported by National Natural Science Foundation of China, No 51175119.

References

Chokkalingham, S., Chandrasekhar, N., & Vasudevan, M. (2011). Predicting the depth of penetration and weld bead width from the infra red thermal image of the weld pool using artificial neural network modeling. *Journal of Intelligent Manufacturing*. doi:10.1007/s10845-011-0526-4.

Davies, O. L. (1978). *The design and analysis of industrial experiments*. New York: Longmen.

Demuth, H., & Beale, M. (1998). *Neural network toolbox-for use with MATLAB*. Natick, MA: The Math Works Inc.

Doumanidis, C., & Kwak, Y. M. (2002). Multivariable adaptive control of the bead profile geometry in gas metal arc welding with thermal scanning. *International Journal of Pressure Vessels and Piping, 79*, 251–262.

Huang, W., & Kovacevic, R. (2011). A neural network and multiple regression method for the characterization of the depth of weld penetration in laser welding based on acoustic signatures. *Journal of Intelligent Manufacturing, 22*, 131–143.

Kannan, T., & Yoganandh, J. (2010). Effect of process parameters on clad bead geometry and its shape relationships of stainless steel claddings deposited by GMAW. *Internal Journal of Advanced Manufacturing Technology, 47*, 1083–1095.

Karunakaran, K.P., Suryakumar, S., Pushpa, V., & Akula, S. (2010). Low cost integration of additive and subtractive processes for hybrid layered manufacturing. *Robotics and Computer-Integrated Manufacturing, 26*, 490–499.

Lin, H. L. (2010). The use of the Taguchi method with grey relational analysis and a neural network to optimize a novel GMA welding process. *Journal of Intelligent Manufacturing.* doi:10.1007/s10845-010-0468-2.

Montgomery, D. C. (2003). *Design and analysis of experiments*. Singapore: Wiley (Asia).

Mughal, M. P., Fawad, H., & Mufti, R. A. (2006). Three-dimensional finite-element modelling of deformation in weld-based rapid prototyping. *Proceedings of the Institution of Mechanical Engineers, Part C: Journal of Mechanical Engineering Science, 220*(6), 875–885.

Murugan, N., & Gunaraj, V. (2005). Prediction and control of weld bead geometry and shape relationships in submerged arc welding of pipes. *Journal of Materials Processing Technology, 168*, 478–487.

Nagesh, D. S., & Datta, G. L. (2002). Prediction of weld bead geometry and penetration in shielded metal-arc welding using artificial neural networks. *Journal of Materials Processing Technology, 123*, 303–312.

Song, Y. A., & Park, S. (2006). Experimental investigations into rapid prototyping of composites by novel hybrid deposition process. *Journal of Materials Processing Technology, 171*, 35–40.

Song, Y. A., Parka, S., & Chae, S. W. (2005). 3D welding and milling: Part II-optimization of the 3D welding process using an experimental design approach. *International Journal of Machine Tools and Manufacture, 45*, 1063–1069.

Sreenathbabu, A., Karunakaran, K. P., & Amarnath, C. (2005). Statistical process design for hybrid adaptive layer manufacturing. *Rapid Prototyping Journal, 11*(4), 235–248.

Unocic, R. R., & DuPont, J. N. (2004). Process efficiency measurements in the laser engineered net shaping process. *Metallurgical and Materials Transactions B, 35B*(1), 143–152.

Weiss, L. E., Prinz, F. B., Adams, D. A., & Siewiorek, D. P. (1992). Thermal spray shape deposition. *Journal of Thermal Spray Technology, 1*(13), 231–237.

Zhang, Y. M., Chen, Y., Li, P., & Male, A. T. (2003). Weld deposition-based rapid prototyping a preliminary study. *Journal of Materials Processing Technology, 135*, 347–357.